Impact of swift heavy ions irradiation on the microstructural and electrochemical properties of vanadium nitride thin films for micro-supercapacitors

Allan Lebreton, Camille Douard, Clara Grygiel, Isabelle Monnet, Charlotte Bodin, Jonathan Coleman, Christophe Lethien, Jérémy Barbé, Thierry Brousse

Electrochimica Acta 539 (2025) 146963

Contents lists available at ScienceDirect

Electrochimica Acta

journal homepage: www.journals.elsevier.com/electrochimica-acta

Impact of swift heavy ions irradiation on the microstructural and electrochemical properties of vanadium nitride thin films for micro-supercapacitors

Allan Lebreton [a,b], Camille Douard [a,b], Clara Grygiel [c], Isabelle Monnet [c], Charlotte Bodin [a], Jonathan Coleman [d], Christophe Lethien [b,e], Jérémy Barbé [a,b,*], Thierry Brousse [a,b,*]

[a] Nantes Université, CNRS, Institut des Matériaux de Nantes Jean Rouxel, IMN, Nantes F-44000, France
[b] Réseau sur le Stockage Electrochimique de l'Energie (RS2E), CNRS FR 3459, 33 rue Saint Leu, Amiens, France
[c] CIMAP, Normandie University, CEA, CNRS, ENSICAEN, UNICAEN, Bd Henri Becquerel, Caen, France
[d] School of Physics, CRANN and AMBER Research Centres, Trinity College Dublin, Dublin 2, Ireland
[e] Institut d'Electronique, de Microélectronique et de Nanotechnologies, Université de Lille, CNRS, Université Polytechnique Hauts-de-France, UMR 8520 - IEMN, Lille F-59000, France

ARTICLE INFO

Keywords:
Swift heavy ions
Supercapacitor
Thin films
Reactive DC magnetron sputtering
Vanadium nitride

ABSTRACT

The role of defects in pseudocapacitive electrode materials has been poorly investigated due to the poor control of their introduction in a pure phase material. Chemical defects are difficult to monitor although it seems they have an obvious influence on the electrochemical properties of the pristine material. The controlled introduction of defects should provide a more rational approach to understand their role in charge storage mechanisms. This study investigates the impact of swift heavy ions irradiation on the electrochemical properties of pseudocapacitive vanadium nitride (VN) thin films, a promising material for micro-supercapacitor electrodes. VN films were irradiated with $^{129}Xe^{19+}$ ions at an energy of 70.95 MeV and a fluences up to 10^{14} ions·cm^{-2}. The effects of irradiation were compared to those observed in a previous study using lower-energy As^{+} ions (20–150 keV) [1]. Scanning electron microscopy (SEM), X-ray diffraction (XRD) and X-ray photoelectrons spectroscopy (XPS) analyses revealed significant structural changes in the irradiated films, including densification, amorphization and oxidation of VN film surface. The electrochemical performance of the irradiated films was evaluated using cyclic voltammetry. While capacitance was reduced at low scan rates, a notable improvement was observed at high scan rates, which is attributed to the increase in electrical conductivity resulting from irradiation. This study deepens our understanding of the effects of high-energy ion irradiation on electrode materials and highlights the potential of this technique as a tool for guiding the development of more efficient energy storage devices.

1. Introduction

Transition metal nitrides (TMNs) such as RuN, CrN, W_2N or TiN have gained significant attention as promising materials for electrochemical capacitors due to their high theoretical capacitance (> 700 F·cm^{-3}) and high electrical conductivity, which enables them to also serve as the current collector in micro-supercapacitors (MSC) [2]. Among these materials, high capacitance value (≈1.4 F·cm^{-2}) was recently demonstrated with sputtered vanadium nitride (VN) films deposited on Si wafer [3]. This thin film electrode also showed high capacitance retention value after 150 000 cycles and high rate capability (75 % of the initial capacitance at 1.6 V·s^{-1}), making it a key candidate as high performance electrode for high-power MSCs.

Recent works have highlighted the importance of controlling the microstructure of VN films to optimize their electrochemical performance. Vacuum deposition methods such as magnetron sputtering provide high flexibility for tuning the morphology and microstructure of TMN pseudocapacitive films, allowing for the evaluation of the structure–property relationships of thin-film materials. For instance, Robert et al. confirmed the role played by the deposition temperature in the growth of pyramidal patterns, and subsequently in optimizing the capacitance and the specific surface [4]. In our recent works, we have explored various methods to control the microstructure and morphology of VN thin films deposited via reactive sputtering. We have shown that

* Corresponding authors at: Nantes Université, CNRS, Institut des Matériaux de Nantes Jean Rouxel, IMN, Nantes F-44000, France.
E-mail addresses: jeremy.barbe@cnrs-imn.fr (J. Barbé), thierry.brousse@cnrs-imn.fr (T. Brousse).

https://doi.org/10.1016/j.electacta.2025.146963
Received 13 May 2025; Received in revised form 8 July 2025; Accepted 19 July 2025
Available online 24 July 2025

adjusting parameters like target power and reactive gas flowrate (both controlling sputtering regimes) [5], thickness [6] or substrate voltage bias [7], significantly affects the charge storage mechanism and overall electrochemical performance of VN thin film electrodes.

The present work builds upon these findings by aiming at modifying the microstructure and create structural defects through a post-deposition technique. Recently, we have used ions implantation at intermediate energy (As^+ with energies ranging from 20 keV up to 150 keV) to improve understanding on how defects contribute to the improvement of the charge storage in such pseudocapacitive material [1]. It was demonstrated that despite lower capacitances at low scan rate, As^+ implanted VN films exhibit better capacitance retention at high scan rate of 100 $mV{\cdot}s^{-1}$. Based on these promising results, we decided to study the irradiation of such materials with higher energy to exacerbate the structural changes and get better insights into the role of defects on electrochemical storage properties.

Irradiation with swift heavy ions (SHI) has recently attracted significant attention as a promising technique for materials nano-engineering. When high-energy ions (typically with a mass ranging from 6 to 239 atomic mass units and energies above 1 MeV per nucleon) impact a material, they transfer an important quantity of energy to the electrons and nuclei of the target, resulting in localized structural modifications and defects. These modifications induced by inelastic energy deposition can be in the form of cylindrical ion tracks with a typical diameter of several nanometers [8], near-surface defects such as nano-hillocks [9,10], or point defects [11].

In the context of thin films, SHI irradiation is particularly useful for altering surface morphology, and inducing microstructural changes, depending on the ion species, energy and fluences used. For example, SHI treatment has been shown to induce amorphization and recrystallization of V_2O_5 thin films for high fluences of 200 MeV Ag^{15+} ions [12]. A significant improvement in electrical transport properties has been ascribed to grain growth with ions irradiation at 5×10^{11} ions·cm^{-2} fluence [13]. In another study, it was shown to induce point defects or clusters in SnO_2 and $Sn_{0.9}Mn_{0.1}O_2$ thin films irradiated with 120 MeV Au^{9+} ions, eventually modifying the bandgap and electrical conductivity of the films [14]. Several other works showed that SHI could modify the electronic properties and optical properties of thin film semiconductors [15], and induce controlled nanostructuring [16]. SHI irradiation could offer a method for producing unique material properties that are not easily attainable through conventional processing techniques. These modifications can be tailored by adjusting ion parameters such as mass, energy and fluence.

In this work, we have used $^{129}Xe^{19+}$ ions with energy of 70.95 MeV to irradiate 350 nm-thick VN thin films with fluence up to 10^{14} ions·cm^{-2}. The microstructural and chemical properties of the films were studied by scanning electron microscopy (SEM), X-ray diffraction (XRD) and X-ray photoelectron spectroscopy (XPS) before and after irradiation. Besides, the electrochemical properties were analyzed by cyclic voltammetry and impedance spectroscopy to reveal the impact and benefit of $^{129}Xe^{19+}$ ions irradiation on electrochemical charge storage properties for high-power devices.

2. Materials and methods

2.1. Reactive sputtering

Sputtering Deposition of VN Thin Film: VN thin films were deposited on silicon wafers with a 500 nm-thermal SiO_2 layer by reactive magnetron sputtering (Ar/N_2) from a pure 4 in vanadium target (99.9 %) using an AV-02 reactor from MHS. The SiO_2 layer is meant to prevent Si etching by KOH electrolyte. Before the deposition, the pressure was kept below 10^{-6} mbar and the target–substrate distance was fixed at 10 cm. During the thin film deposition, target power, discharge pressure, argon and nitrogen flow rates were fixed, respectively, at 300 W, 5×10^{-3} mbar, 80 sccm and 1.6 sccm. The substrate was not intentionally heated although it could heat up slightly during deposition. The deposition time was fixed at 3 h in order to obtain samples with thicknesses of approximately 350 nm. Although there is no intentional introduction of molecular O_2 in the reactor, films contain a significant fraction of oxygen, which is explained by oxidation during exposure to air, due to the high getter property of vanadium and porosity of the films. This is why the obtained VN thin films also contain a significant fraction of amorphous vanadium oxide. Previous results suggest that the films are composed of two distinct phases: vanadium nitride in the bulk and vanadium oxides at the surface [5].

2.2. Swift heavy ions bombardment in GANIL

The samples were irradiated at GANIL accelerator (Caen, France), on the IRRSUD line, with $^{129}Xe^{19+}$swift heavy ions of 70.95 MeV. Ion irradiation was carried out under normal incidence, at room temperature, and with a fluence ranging from 1.10^{13} ions·cm^{-2} to 1.10^{14} ions·cm^{-2}. Flux was kept under 5.10^9 ions·cm^{-2} in order to avoid macroscopic sample heating.

2.3. Thin film characterization

Room temperature XRD data were obtained using a Bruker “D8 Advance” diffractometer operated in Bragg-Brentano geometry with a Cu anode sealed X-ray tube and a focusing Ge(111) primary monochromator (selecting the Cu Kα1 radiation; $\lambda = 1.540598$ Å). We used a 1-D silicon-strip position sensitive detector (“LynxEye” detector) with an active area of 3.7° 2Θ (goniometer radius: 217.5 mm).

XRD grazing incidence were obtained on a Bruker “D8 Advance” diffractometer with 1° incidence angle in parallel beam (parabolic mirrors and equatorial slits) in mode 0D

SEM measurements were conducted on a ZEISS Merlin instrument with secondary electron detector.

XPS measurements were conducted on a Kratos Axis Ultra Instrument, using a monochromated Al Kα source (1486.6 eV) operating at 225 W. Wide range spectra were realised prior to core level measurements of the different elements detected with pass energy of 80 eV. The pass energy and the step scan to measure the region of interest were fixed to 40 eV and 0.1 eV, respectively. The typical probed depth was 10 nm over a 700×300 μm^2 zone. The dwell time and number of sweeps were chosen such as the highest XPS peak of the selected zone exhibits, at least, 100 000 counts. Charge neutralization was used when acquiring the spectra. The energy calibration was set from C1s signal allotted to adventitious carbon (C—C bonds) fixed at 284.9 eV. Using CasaXPS software, the elemental composition was determined from the area under C1s, O1s, V2p and N1s peaks after removal of a Shirley-type background.

Conductivity measurement were performed by four-points probe method using a pro4 device from Lucas Labs connected with a Keithley 3601A system source-meter. The software used to run those experiments was Pro4 and the measurements were performed applying a current of 10 mA with a 5 % tolerance.

2.4. Electrochemical measurements

Aqueous electrochemical measurements were performed in 1 M KOH aqueous electrolyte using three electrode cell [17]. Hg/HgO was used as reference electrode and a platinum wire as the counter electrode. Nitrogen bubbling was carried out prior to measurement to eliminate dissolved O_2 from the electrolyte. The potential window was fixed between −1 V and −0.4 V vs Hg/HgO reference electrode to avoid any side reaction and/or additional sample degradation.

VMP3 potentiostat/galvanostat (Biologic) monitored by EC-lab software, was used for data collection and data treatment. The protocol to analyse the electrochemical properties was the same for all samples: (i) 50 activation cycles at 20 $mV{\cdot}s^{-1}$ were performed before

measurements. (ii) CV measurements were realised with scan rates ranging from 5 to 10 000 $mV{\cdot}s^{-1}$ in aqueous media. All measurements were conducted at a temperature of 295 K.

Electrochemical impedance spectroscopy (EIS) measurements were performed with a AC signal with an amplitude of 10 mV between 100 mHz and 1 MHz at open circuit voltage (OCV).

3. Results and discussion

To estimate the penetration depth and the lateral deviation of $^{129}Xe^{19+}$ ions, simulations were performed using the SRIM-TRIM software. The simulation results are shown in Fig. 1. The silicon layer is included solely to illustrate the trajectory of the ions after passing through the vanadium nitride layer. These results were obtained through simulations with 1000 ions with energy fixed at 70.95 MeV, and the density of the vanadium nitride layer was set to 4.5 $g{\cdot}cm^{-3}$. This value was determined by weighing the sample before and after VN deposition, knowing the exact surface and thickness of the thin film.

The penetration depth and lateral dispersion are primarily determined by two factors: the atomic mass and the energy of the ions. As shown in Fig. 1(b), the distribution of the stopping depth of the bombarded ions is quite narrow and centered around 11.4 µm. It can therefore be stated that the vast majority of implanted ions will pass through the 300–350 nm vanadium nitride layer and stop in the underlying substrate.

Fig. 1(b) also shows a lateral dispersion of 570 nm, which is relatively narrow. As compared to conventional ions implantation, the ions possess very high energy, and during an inelastic collision with another nucleus, the $^{129}Xe^{19+}$ ion will experience only minimal deviation, whereas the encountered target will absorb a large amount of energy through electronic excitations inducing cylinders of modified materials called latent tracks. Bombardment with heavy and energetic ions thus generates numerous structural defects along the entire ion path within the bombarded material. The extent of the damage depends on the materials properties and beam parameters, and increases with ion fluences. The electronic stopping power, defined as the inelastic energy dissipated per unit of penetration depth, is calculated to be 23 $keV{\cdot}nm^{-1}$. As the stopping power is significantly high, the defects created by this bombardment are expected to be significant.

SEM observations of as-deposited and irradiated VN thin films were performed at the surface and cross-section for various ions fluences (Fig. 2), in order to observe the morphological changes induced by ion bombardment.

For the surface images, two major developments are observed with increasing ion bombardment fluences. The main change corresponds to the formation of surface cracks that grow with ion fluences. These cracks indicate the presence of stress and could be indicative of film

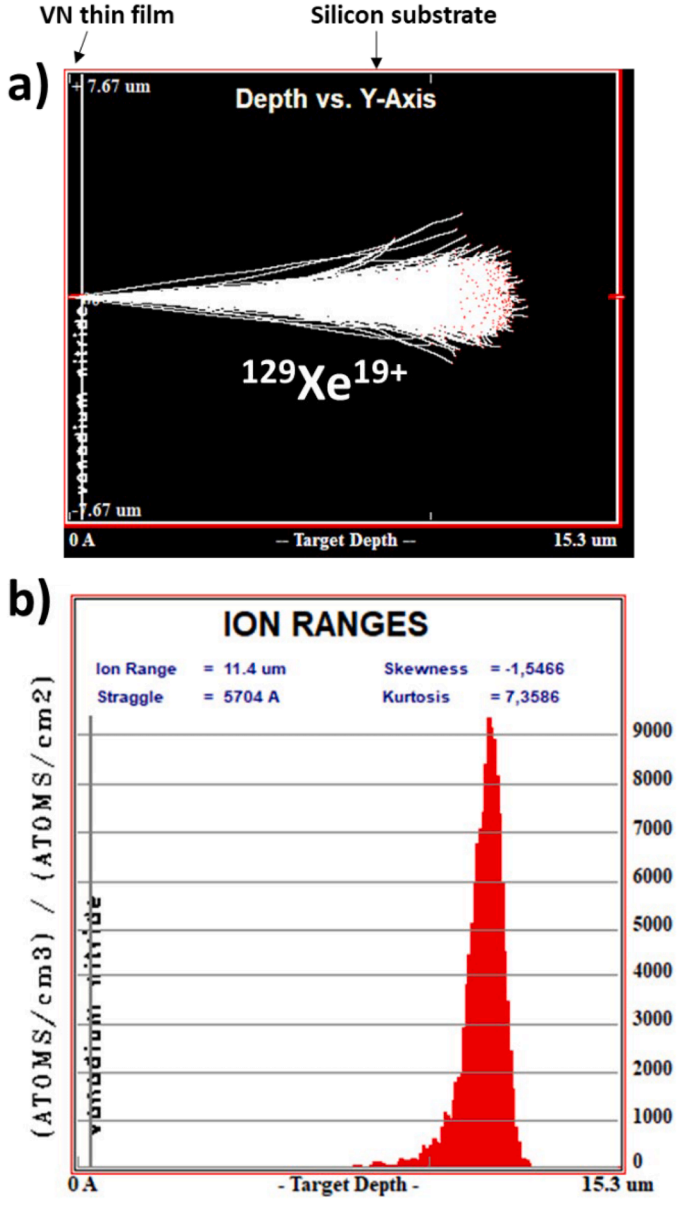

Fig. 1. (a) SRIM/TRIM simulated trajectory distribution of $^{129}Xe^{19+}$ ions with energy 70.95 MeV implanted into a VN thin film deposited on a silicon substrate. (b) Depth profile of ions implantation, showing the distribution of implanted $^{129}Xe^{19+}$ ions as a function of depth. The mean implantation depth is 11.4 µm.

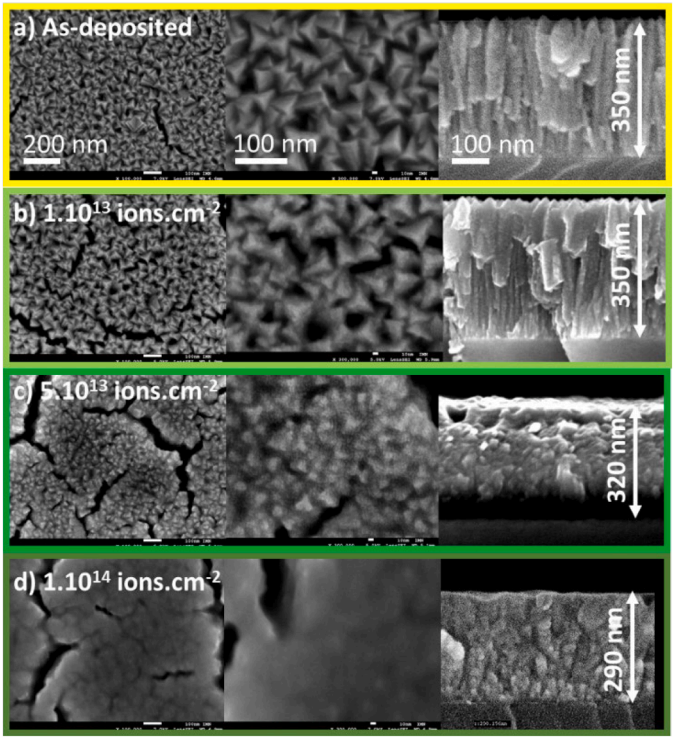

Fig. 2. SEM micrographs of VN thin films deposited on silicon substrates subjected to different $^{129}Xe^{19+}$ ions bombardment fluences. The micrographs show the surface morphology (left), zoomed-in surface features (middle), and cross-sectional views (right) of (a) as deposited sample (no bombardment, ~350 nm thick); (b) 1×10^{13} $ions{\cdot}cm^{-2}$ (~350 nm); (c) 5×10^{13} $ions{\cdot}cm^{-2}$ (~320 nm); (d) 1×10^{14} $ions{\cdot}cm^{-2}$ (~290 nm, severe cracks and amorphization).

compaction caused by the bombardment. The second change is related to the disappearance of the pyramidal structures present on the surface of the as-deposited VN sample, resulting in a much smoother morphology for the sample bombarded at 1×10^{14} ions·cm^{-2}.

From the cross-sectional images (on the right), the columnar microstructure is significantly altered after irradiation above 1×10^{13} ions·cm^{-2}. Samples irradiated at 5×10^{13} ions·cm^{-2} and 1×10^{14} ions·cm^{-2} present a granular structure indicating a loss of preferential orientation after irradiation at high fluences, due to the change of columnar growth to granular growth. Besides, a reduction in the layer thickness, from 350 nm for the reference sample to 290 nm for the sample bombarded with a fluence of 1×10^{14} ions·cm^{-2} is observed, which agrees with a densification of the film. It can be noted that at such fluence the recovering of the latent tracks of SHI is likely to occur.

To investigate whether ion bombardment causes variations in the crystalline properties of the samples, X-ray diffraction measurements were conducted using both Bragg-Brentano and grazing angle configurations.

Fig. 3(a) presents the Bragg-Brentano diffractograms of the VN samples. These samples exhibit only one peak at 37.6°, indicating a preferential texturing of the films along the (111) orientation. A decrease in the intensity of this peak along with an increase in full width at half maximum (FWHM), from 0.38° for the as-deposited sample to 1.17° for the sample irradiated with a fluence of 1×10^{14} ions·cm^{-2}, confirm the loss of crystallinity of the films as the irradiation fluence increases, as suggested by the SEM analysis.

The diffractograms obtained in grazing angle configuration are shown in Fig. 3(b). A shift of the peaks corresponding to the (111) and (220) orientations of VN to higher angles is observed, indicating the presence of compressive stresses, which agrees with the hypothesis of film compaction during irradiation. For the sample bombarded with a fluence of 1×10^{14} ions·cm^{-2}, a peak at 44° corresponding to (200) orientation is detected. The growth of the peak near 55.5° is not quite understood but may be assigned to (220) orientation of VO_2 (JCPDS 01–071–1421) or (112) orientation of $V_2N_{0.9}$ (JCPDS 00–030–1420).

In conclusion, the analysis of the SEM images combined with the X-ray diffraction measurements strongly supports the hypothesis of thin film densification, decrease of crystallinity, the formation of compressive stresses and formation of oxide phases with increasing ion irradiation fluence.

Next, to assess the changes in electronic properties of VN films due to ions irradiation, the in-plane electronic conductivity was measured by using a four-point probe (Fig. 4). An increase in the conductivity with increasing ion fluences is observed. The conductivity increases from 250 S·cm^{-1} for the as-deposited sample to 2080 S·cm^{-1} for the sample irradiated at a fluence of 1×10^{14} ions·cm^{-2}. It appears that the densification of the samples induced by irradiation contributes to the increase in the in-plane electronic conductivity of the samples. This result is in perfect agreement with our previous work, which demonstrated that increasing substrate polarisation during VN deposition resulted in a densification of the film due to atomic peening effect, and eventually to an increased in-plane electronic conductivity [7].

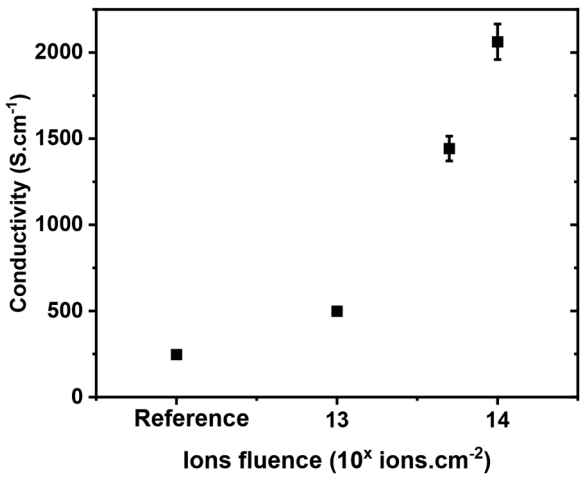

Fig. 4. four-point probe conductivity measurements of VN thin films irradiated at various $^{129}Xe^{19+}$ ions fluences.

To further highlight the changes in surface chemistry due to swift heavy ions irradiation, the surface elemental composition of VN thin films was studied using X-ray photoelectron spectroscopy (XPS). The wide scan spectrum shown in Fig. 5(a) reveals the presence of vanadium, carbon, nitrogen, and oxygen at the sample surface. The surface composition as a function of $^{129}Xe^{19+}$ ion fluences is shown in Fig. 5(b). The vanadium and carbon contents appear stable at approximately 16 at. % and 30 at. %, regardless of ion fluences. Carbon is mainly due to surface contamination during air exposure of the sample. However, a trend is observed for the ratio of nitrogen and oxygen as a function of ion fluences. The nitrogen content decreases from 15 % to 7 %, while the oxygen content increases from 37 % to 45 % with increasing ion fluences. Thus, the bombardment of $^{129}Xe^{19+}$ ions induces significant surface oxidation of vanadium nitride. This aligns with previous studies demonstrating that ion irradiation in the MeV range can induce oxidation in metallic titanium samples [18]. However, to the best of our knowledge, this is the first report of surface oxidation of a nitride thin film due to ions irradiation.

Hence, the bombardment of $^{129}Xe^{19+}$ ions induces significant oxidation of the surface of vanadium nitride films. To better understand the chemical modifications induced by ion bombardment, the V2p 3/2 core-level peak was deconvoluted (Fig. 6a-d) following the work of Biesinger et al. [19]. This deconvolution is based on four different components related to the oxidation states of vanadium in VN, V_2O_3, VO_2 and V_2O_5. However, as the V_2O_3 (V^{3+}) and VO_2 (V^{4+}) components are difficult to separate with accuracy, and could lead to potential errors, we merged these two components into one component (V^{3+}/V^{4+}) in the

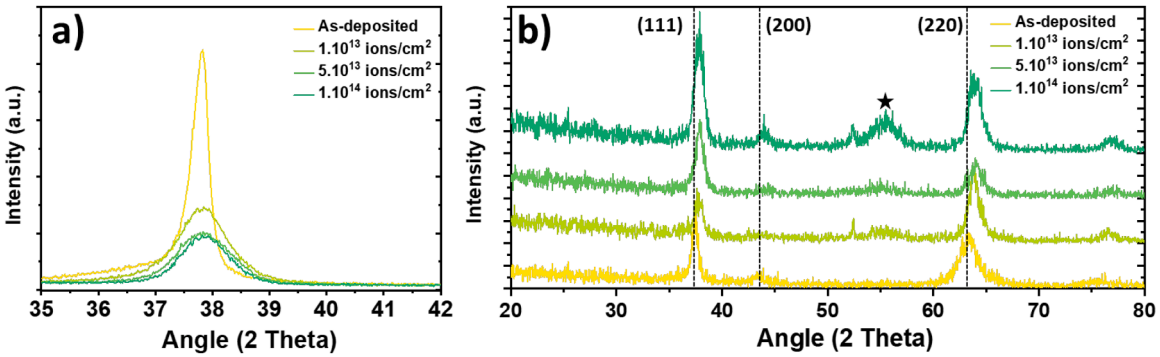

Fig. 3. XRD patterns of VN thin films under different $^{129}Xe^{19+}$ ion bombardment fluences, measured in (a) Bragg-Brentano configuration and (b) grazing incidence.

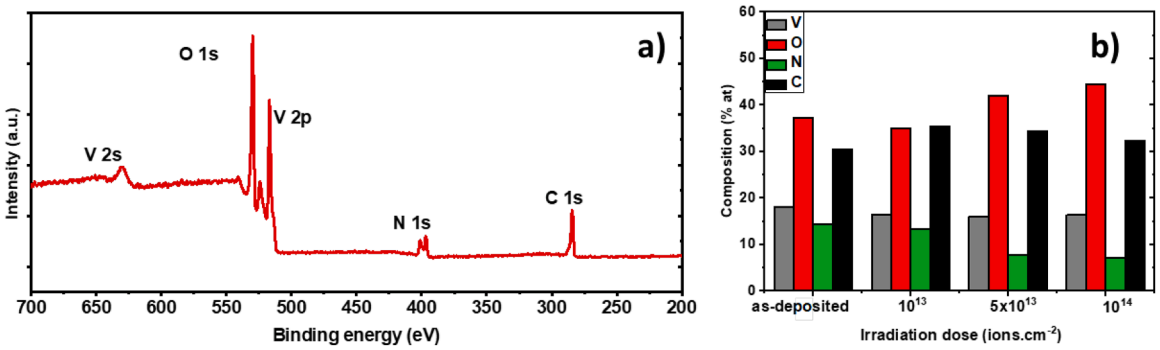

Fig. 5. (a) XPS wide spectrum of vanadium nitride thin films bombarded with $^{129}Xe^{19+}$ ions at different fluences. (b) Histograms of elemental compositions for various ion fluences (%at.).

range 515–516.4 eV, with a relatively high FWHM of 2–3 eV. The position, FWHM and area of the three components were fit to the measured data.

Based on this decomposition, the evolution of the different components with ion fluences is presented in Fig. 6(e). The component located around 513.9 eV, attributed to VN, disappears as the irradiation fluence increases. This is accompanied by an increase in the component attributed to V^{5+} (V_2O_5), which rises from 45 % for the as-deposited VN thin film to >63 % for the sample irradiated at 10^{14} ions·cm^{-2}. The intermediate oxidation state (V^{3+}/V^{4+}) remain rather stable. Therefore, it appears that the surface oxidation of vanadium nitride due to ion bombardment leads to the complete disappearance of vanadium nitride at the surface in favor of V_2O_5, which becomes the dominant specie at fluences $\geq 5 \times 10^{13}$ ions·cm^{-2}. It is believed that the oxidation of the VN film would occur primarily at the surface and has little effect on the in-plane conductivity, whereas the densification of the film has a more significant impact.

Based on the analysis of materials properties, preliminary findings suggest that the primary effects of heavy ion irradiation on VN thin films are (i) densification of the film linked to the irradiation, (ii) amorphisation of the film, identified by both SEM and XRD measurement, (iii) oxidation of the surface and increase in V^{5+} oxidation states, revealed by GI-XRD and XPS measurements.

To assess how these alterations affect the electrochemical properties of VN pseudocapacitive thin films, several characterizations in 1 M KOH electrolyte were conducted.

Figs. 7a-d show the cyclic voltammetry of VN films from 1 mV·s^{-1} to 1 000 mV·s^{-1}. At cycling rates of 1 mV·s^{-1} and 10 mV·s^{-1}, the as-deposited sample displays the typical electrochemical signature of vanadium nitride, i.e. a rectangular envelope characteristic of pseudocapacitive materials, coupled with a pair of redox peaks centered at −0.65 V vs. Hg/HgO due to intercalation processes [3]. The sample bombarded with $^{129}Xe^{19+}$ ions at a fluence of 1×10^{13} ions·cm^{-2} shows a similar shape, with a slight decrease in the area under the curve, indicating a slight reduction in stored charge. Samples bombarded at higher fluences (5×10^{13} ions·cm^{-2} and 1×10^{14} ions·cm^{-2}) exhibit only a pseudocapacitive behavior (rectangular envelope without redox peaks), with a significantly reduced area.

At 100 mV·s^{-1} (Fig. 7c), both the as-deposited sample and the one bombarded at a fluence of 1×10^{13} ions·cm^{-2} show a "rugby ball" shape, indicating the transition between capacitive to resistive behavior of the VN thin film. Samples irradiated at higher fluences still show pseudocapacitive behavior, with a relatively small area under the curve.

Finally, at 1000 mV·s^{-1} (Fig. 7d), the as-deposited samples and the one bombarded at a fluence of 1×10^{13} ions·cm^{-2} exhibit fully resistive behavior, while samples irradiated at higher fluences only begin to show the transition between capacitive and resistive behavior.

These results highlight two key trends. First, at low cycling rates a decrease in the maximum stored charge and loss of redox peaks are observed after ions irradiation. Second, improved performance at high cycling rates is seen in samples bombarded at high fluences ($\geq 5 \times 10^{13}$ ions·cm^{-2}). To explain the evolution of capacity in relation to irradiation fluence at both low and high cycling rates, it is essential to consider the effects of microstructure (specifically surface area) and surface oxidation states.

In one of our previous papers [4], we demonstrated that the ion intercalation charge storage mechanism (faradic mechanism) is driven by the V^{4+}/V^{3+} redox couple:

$$V^{4+}O_2 + H_2O + 2e^- \rightarrow V^{3+}OOH + OH^-$$

On one hand, at low cycling rates, Fig. 7 shows that the intercalation peaks disappear after irradiation at high fluence (5×10^{13} and 10^{14} ions cm^{-2}), which can be attributed to changes in surface chemistry and oxidation states. As shown in Fig. 6, the V^{5+} oxidation state increases from 40 % to >60 % after irradiation. This suggests that the presence of V^{5+} could inhibit ion intercalation. Additionally, at low cycling rates, we observe a decrease in electric double-layer capacitance (EDLC) and pseudocapacitance charge storage mechanisms. This is likely due to the increased density of the film and the reduction in specific surface area after irradiation at high ion fluence.

On the other hand, the improved performance at high cycling rates after ions irradiation with high fluence would be directly linked to the increase of the in-plane conductivity as illustrated in Fig. 4. Indeed, at high cycling rates, the accessibility of electrons to the electrode (i.e., the electrical conductivity) becomes more critical. This suggests that at high cycling rates, it may be more important to enhance conductivity, even if the specific surface area is reduced. Similar observations were already reported in previous work regarding the effect of substrate polarisation [7].

In the next part, a fitting model was used to determine the maximum capacity, characteristic time associated with charge/discharge and capacity decay slope at high cycling rate for each ions fluence. This method consists principally in fitting the capacity vs. scan rate plots, using Eq. (1). In this equation, Q_{exp} corresponds to the measured charge, Q_m (mC.cm^{-2}) to the maximum charge at low scan rates and R to the rate in cycle·h^{-1}. τ_{fit} is the characteristic time associated with charge/discharge of the sample in h·cycle^{-1} and finally n is the power law decay at high cycling rates.

$$Q_{exp} = Q_m\left[1 - \left(R\tau_{fit}\right)^n\left(e^{-\left(R\tau_{fit}\right)^{-n}}\right)\right] \quad (1)$$

with $R = \frac{I}{Q_{exp}}$ (2). The results are displayed in Fig. 8a and all plots present very good fit. The evolution of the factor n, which describes the origins of limitations at high cycling speed, is shown in Fig. 8b It was previously described that the n value should be close to 0.5 for diffusion limited systems and 1 for resistance limited systems [20]. Here, a n value of 1 is measured for the as-deposited sample and the sample bombarded with a fluence of 1×10^{13} ions·cm^{-2}, suggesting that the factor limiting the high-rate cycling is the electronic conductivity of the VN thin film, as no current collector is used here (VN is used both as the active material

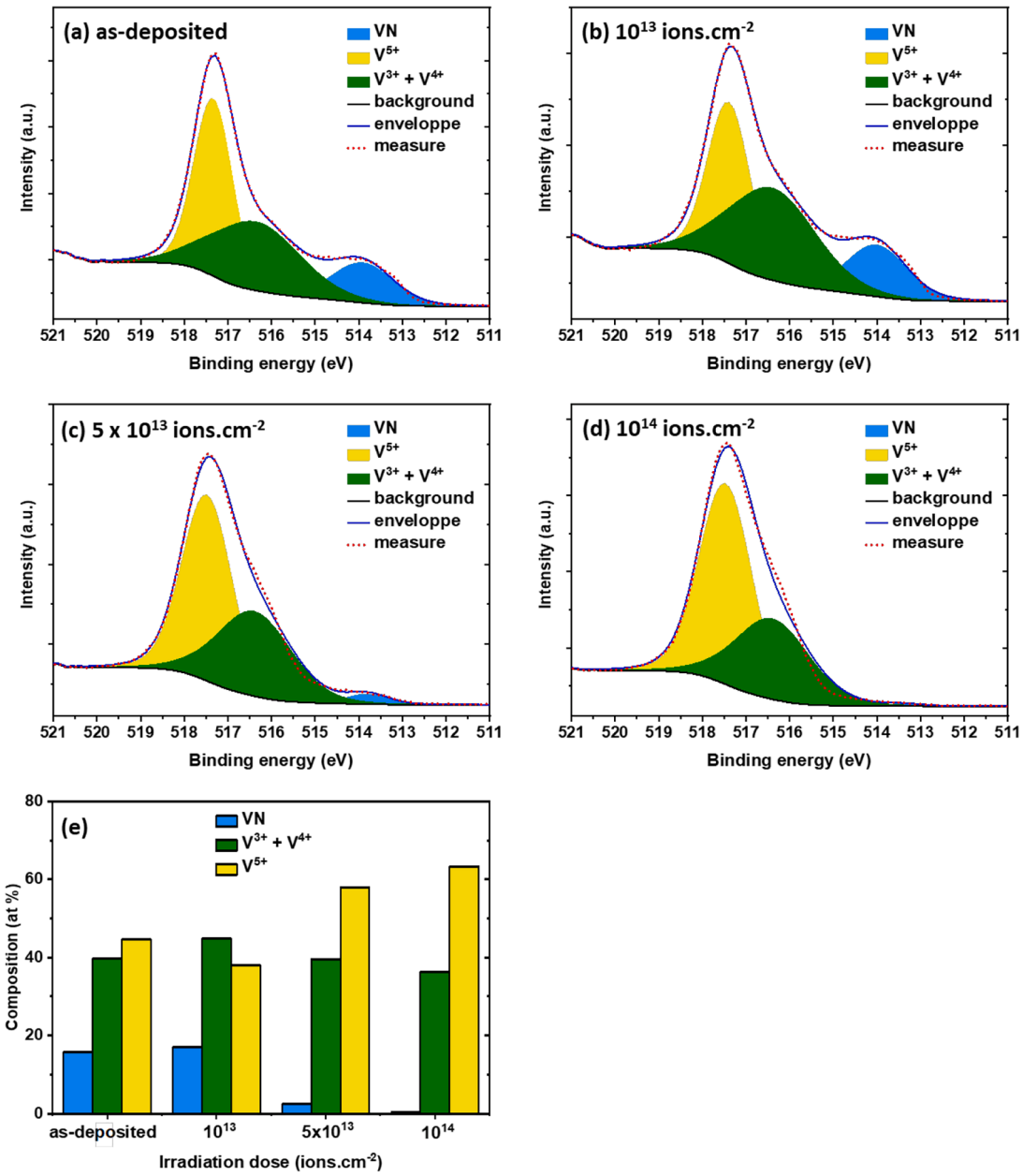

Fig. 6. XPS spectra and compositional analysis of VN thin films as a function of ions irradiation fluences. (a–d) High-resolution XPS spectra of the V2p 3/2 core level: (a) as-deposited, (b) irradiated at 10^{13} ions·cm^{-2}, (c) irradiated at 5×10^{13} ions·cm^{-2}, and (d) irradiated at 10^{14} ions·cm^{-2}. Deconvolution shows contributions from VN (blue), $V^{3+} + V^{4+}$ (green), and V^{5+} (yellow). (e) Compositional evolution of VN, $V^{3+} + V^{4+}$, and V^{5+} species as a function of ions irradiation fluence, highlighting changes in the chemical states of vanadium.

and current collector thanks to its high electronic conductivity). For samples bombarded at higher fluences, the value of n becomes unreliable as the slope at high cycling rates is scarcely observed and fit. In this case, fits were performed with a value n fixed to 1, without conclusions made on high-speed cycling limitations from these fits.

The evolution of the characteristic charge/discharge time τ, determined through fits (τ_{fit}) and EIS (τ_{EIS}) plots, is shown in Fig. 8c [7]. This value describes the time at which the sample presents a switch from capacitive/pseudocapacitive to resistive behaviour, and should be minimized to achieve fast electrochemical storage devices. The time constant for the pristine and lightly irradiated sample (10^{13} ions cm^{-2}) is close to 10 s, whereas this value decreases to below 1 s for the films irradiated at 5×10^{13} and 10^{14} ions cm^{-2}. This decrease is consistent with the increase in sample conductivity due to changes in microstructure and composition after irradiation, and suggests that irradiated thin films have lower rate limitations

Finally, the evolution of the maximum stored charge for these samples is shown in Fig. 8d A significant decrease in the maximum stored charge is observed, decreasing from 19 mC·cm^{-2} for the reference sample to <3 mC·cm^{-2} for the sample bombarded with a fluence of 1×10^{14} ions·cm^{-2}. This reduction in maximum stored charge appears to be related to the microstructural and chemical changes presented earlier.

These results should be discussed in parallel with our previous investigations of the impact of substrate polarization during the deposition of VN thin films [7]. We had shown that increasing the polarization led to the densification of the films through an atomic peening effect. This densification, along with the associated structural changes, resulted in increased in-plane electrical conductivity, and ultimately higher capacity at high cycling speeds. The main conclusion of this previous study was that porous crystalline thin films offer high capacity at low cycling

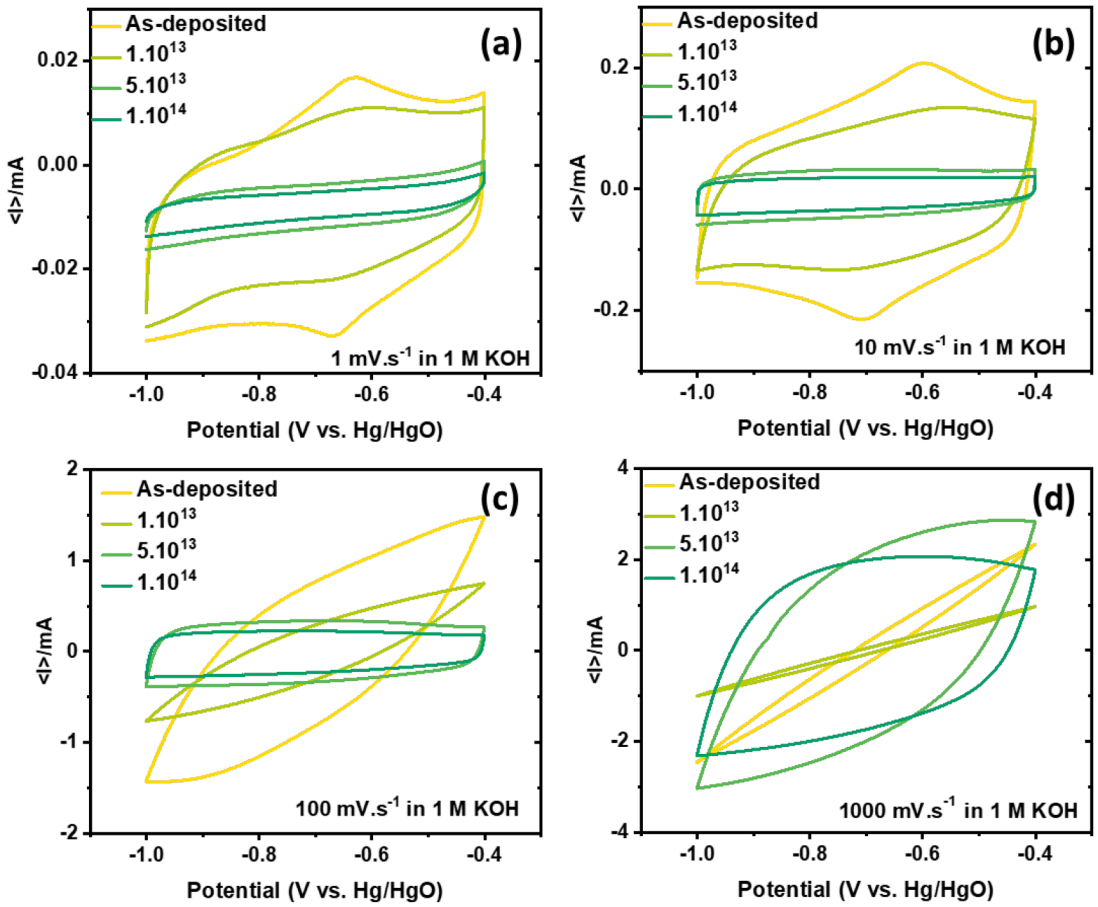

Fig. 7. Cyclic voltammograms of 350 nm thick vanadium nitride thin films in 1 M KOH, bombarded with $^{129}Xe^{19+}$ ions at different fluences and cycling speeds of a) 1 mV·s^{-1}, b) 10 mV·s^{-1}, c) 100 mV·s^{-1}, and d) 1000 mV·s^{-1}.

rate due to their high specific surface area, while dense amorphous films exhibit lower characteristic times associated with charge/discharge due to their higher electronic conductivity, and thus higher capacity at fast cycling rate. Therefore, a trade-off between optimized capacity and characteristic time for charge/discharge could be achieved by adjusting the substrate bias voltage. In the current study, the conclusions follow a similar trend. The main difference lies in the method used to modify the microstructure. Here, a post-deposition process — ions irradiation with highly energetic ions—is employed to modify the microstructure, whereas in the previous study the microstructure was modified directly during deposition through magnetron sputtering. However, both studies show the impact of VN thin film microstructure and electrical resistance on rate performance limitations.

Besides, the current results are in line with our study on arsenide cation (As^+) implantation with energies from 20 keV to 150 keV [21], and fluence of 10^{15} ions·cm^{-2}. Using As^+ ions, it was calculated that ions were mostly implanted in the film. Despite lower capacitance was achieved at low scan rate (2 mV·s^{-1}), As^+ implanted VN films exhibited better capacitance at high scan rate (100 mV·s^{-1}). However, no clear microstructural or morphological change was observed by SEM or XRD analysis. In the present study, $^{129}Xe^{19+}$ ions with a substantially higher energy of 70.95 MeV were used. Unlike the As^+ ions, most of these high-energy ions penetrated through the 300–350 nm vanadium nitride layer and were implanted in the underlying substrate. This distinction indicates that the observed changes in the electrochemical performance of the VN film are primarily attributed to defects and modifications induced by the passage of these ions, rather than the implanted ions themselves.

Significant structural alterations were observed through SEM and XRD analyses, revealing more pronounced defects compared to the As^+ implantation study. Despite these differences, the main conclusions remain consistent with our previous findings: capacitance of irradiated films is lower at low scan rate but clearly improved at fast cycling rate. Using high-energy ions and high fluence allows here to amplify the effect of irradiation and brings better understanding on its effect: irradiation induces densification and amorphization of the VN film, and consequently an increase in the electrical conductivity. As VN acts both as an electrode and current collector, this increased conductivity allows to access faster scan rate without losing too much capacitance.

4. Conclusion

As a conclusion, $^{129}Xe^{19+}$ ions irradiation with high energy was used as a novel method to nanostructurate vanadium nitride thin films. In this study, it appears that ions irradiation on VN thin films leads to significant structural, chemical, and electrochemical modifications for irradiation fluence $\geq 5 \times 10^{13}$ ions·cm^{-2}. SEM, XRD and XPS measurements show that ions irradiation induces densification, amorphization, and surface oxidation, favouring the formation of higher oxidation state vanadium oxides such as V_2O_5 and disappearance of VN at high fluences. Besides, ions irradiation induces a clear increase in the electrical conductivity of the films as a result of densification, similarly to what was shown in previous work on the influence of substrate polarisation during thin film deposition [7].

All these microstructural changes have strong impact on the electrochemical performance of VN electrodes. While as-deposited VN shows superior capacity at low cycling rates due to its porous and crystalline microstructure, the irradiated VN electrodes demonstrate

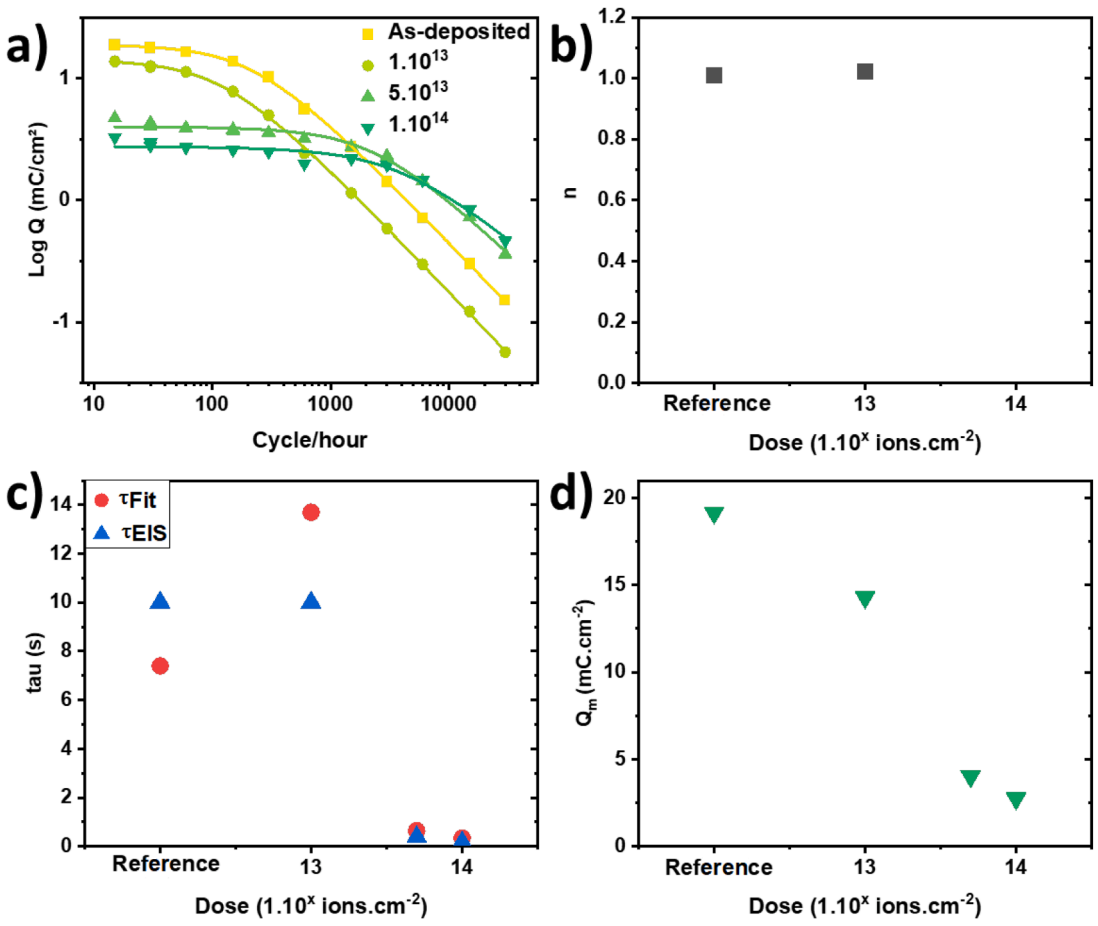

Fig. 8. (a) Areal charge vs. scan rate of vanadium nitride thin films in 1 M KOH bombarded with $^{129}Xe^{19+}$ ions at different fluences. Curves are fitted using Eq. (1). (b) Evolution of n value vs. bombardment fluence determined from the fit. (c) Evolution of the characteristic time τ associated with charge/discharge determined by EIS (in blue triangles) and fitting (in red circles) vs. ion fluences. (d) Evolution of maximum areal charge Q_m vs. ion fluences determined from the fit.

improved capacity retention and faster charge/discharge capabilities at high cycling rates, with still impressive capacitance retention even at very fast scan rates of 1 $V{\cdot}s^{-1}$ or even more. This improvement is attributed to the increased electrical conductivity and thus reduced characteristic time of the irradiated VN, resulting from the structural changes induced by ion irradiation.

Together, these findings highlight the dual role of ion irradiation: as a tool to modify and optimize the material properties of VN thin films and as a method to tailor their electrochemical performance for specific applications. This study provides a foundation for further exploration of ion-irradiated thin films electrode in advanced energy storage devices.

CRediT authorship contribution statement

Allan Lebreton: Writing – review & editing, Writing – original draft, Investigation, Data curation. **Camille Douard:** Writing – review & editing. **Clara Grygiel:** Writing – review & editing, Validation, Methodology. **Isabelle Monnet:** Writing – review & editing, Validation, Methodology. **Charlotte Bodin:** Writing – review & editing. **Jonathan Coleman:** Writing – review & editing, Methodology. **Christophe Lethien:** Writing – review & editing, Supervision. **Jérémy Barbé:** Writing – review & editing, Writing – original draft, Validation, Supervision, Methodology, Investigation, Conceptualization. **Thierry Brousse:** Writing – review & editing, Writing – original draft, Validation, Supervision, Project administration, Methodology, Investigation, Funding acquisition, Conceptualization.

Declaration of competing interest

The authors declare that they have no known competing financial interests or personal relationships that could have appeared to influence the work reported in this paper.

Acknowledgements

Labex STORE-EX (ANR-10-LABX-76–01) and Conseil Régional des Pays de la Loire are acknowledged for financial support (PhD grant AL). The research conducted in this publication was jointly funded by the Irish Research Council (IRC), the French Ministries of Europe and Foreign Affairs (MEAE) and Higher Education and Research (MESR) under grant PHC (Partenariat Hubert Curien) Ulysses 2022 entitled "Quantifying the factors limiting rate performance in supercapacitor electrodes"). Part of this work was performed within the framework of the HIPOHYBAT project funded by the “France 2030″ government investment plan managed by the French Research Agency, under the reference “ANR-22-PEBA- 0003”. The authors would also like to acknowledge Labex STORE-EX (ANR-10-LABX-76–01).

Data availability

Data will be made available on request.

References

[1] E. Le Calvez, D. Yarekha, L. Fugère, K. Robert, M. Huvé, M. Marinova, O. Crosnier, C. Lethien, T. Brousse, Influence of ion implantation on the charge storage mechanism of vanadium nitride pseudocapacitive thin films, Electrochem. Commun. 125 (2021) 0–4.

[2] H.Dinh Khac, G. Whang, A. Iadecola, H. Makhlouf, A. Barnabé, A. Teurtrie, M. Marinova, M. Huvé, I. Roch-Jeune, C. Douard, T. Brousse, B. Dunn, P. Roussel, C. Lethien, Nanofeather ruthenium nitride electrodes for electrochemical capacitors, Nat. Mater. 23 (2024) 670–679.

[3] A. Jrondi, G. Buvat, F.D. La Pena, M. Marinova, M. Huvé, T. Brousse, P. Roussel, C. Lethien, Major improvement in the cycling ability of pseudocapacitive vanadium nitride films for micro-supercapacitor, Adv. Energy Mater. 2203462 (2023) 1–16.

[4] K. Robert, D. Stiévenard, D. Deresmes, C. Douard, A. Iadecola, D. Troadec, P. Simon, N. Nuns, M. Marinova, M. Huvé, P. Roussel, T. Brousse, C. Lethien, Novel insights into the charge storage mechanism in pseudocapacitive vanadium nitride thick films for high-performance on-chip micro-supercapacitors, Energy Environ. Sci. 13 (2020) 949–957.

[5] A. Lebreton, M.-P. Besland, P.-Y. Jouan, T. Signe, C. Mannequin, M. Richard-Plouet, M.Le Granvalet, C. Lethien, T. Brousse, J. Barbé, Control of microstructure and composition of reactively sputtered vanadium nitride thin films based on hysteresis curves and application to microsupercapacitors, J. Vac. Sci. Technol. A. 42 (2024).

[6] A. Lebreton, J. Barbé, C. Lethien, J.N. Coleman, T. Brousse, Tuning deposition conditions for VN thin films electrodes for microsupercapacitors : influence of the thickness, J. Electrochem. Soc. 171 (2024).

[7] A. Lebreton, J. Barbé, C. Lethien, J.N. Coleman, T. Brousse, Tuning deposition conditions for VN thin films electrodes for microsupercapacitors: influence of the substrate bias voltage, J. Electrochem. Soc. 172 (2025).

[8] A. Ibrayeva, A. Mutali, J. O'Connell, A.J. van Vuuren, E. Korneeva, A. Sohatsky, R. Rymzhanov, V. Skuratov, L. Alekseeva, I. Ivanov, Swift heavy ion tracks in nanocrystalline $Y_4Al_2O_9$, Nucl. Mater. Energy. 30 (2022) 101106.

[9] F. Aumayr, S. Facsko, A.S. El-Said, C. Trautmann, M. Schleberger, Single ion induced surface nanostructures: a comparison between slow highly charged and swift heavy ions, J. Phys. Condens. Matter. 23 (2011) 393001.

[10] J.H. O'Connell, G. Aralbayeva, V.A. Skuratov, M. Saifulin, A. Janse Van Vuuren, A. Akilbekov, M. Zdorovets, Temperature dependence of swift heavy ion irradiation induced hillocks in TiO_2, Mater. Res. Express. 5 (2018).

[11] A. Abdullaev, K. Sekerbayev, R. Rymzhanov, V. Skuratov, J.O. Connell, B. Shukirgaliyev, A. Kozlovskiy, Y. Wang, Z. Utegulov, Impact of swift heavy ion-induced point defects on nanoscale thermal transport in ZnO, Mater. Res. Bull. 175 (2024) 112786.

[12] R. Rathika, M. Kovendhan, D.P. Joseph, R. Pachaiappan, A.S. Kumar, K. Vijayarangamuthu, C. Venkateswaran, K. Asokan, S.J. Jeyakumar, Tailoring the properties of spray deposited V_2O_5 thin films using swift heavy ion beam irradiation, Nucl. Eng. Technol. 52 (2020) 2585–2593.

[13] P. Mallick, C. Rath, J. Prakash, D.K. Mishra, R.J. Choudhary, D.M. Phase, A. Tripathi, D.K. Avasthi, D. Kanjilal, N.C. Mishra, Swift heavy ion irradiation induced modification of the microstructure of NiO thin films, Nucl. Instruments Methods Phys. Res. B 268 (2010) 1613–1617.

[14] S. Gupta, F. Singh, N.P. Lalla, B. Das, Swift heavy ion irradiation induced modifications in structural, microstructural, electrical and magnetic properties of Mn doped SnO_2 thin films, Nucl. Instruments Methods Phys. Res. B 400 (2017) 37–57.

[15] B. Dou, E.M. Miller, J.A. Christians, E.M. Sanehira, T.R. Klein, F.S. Barnes, S. E. Shaheen, S.M. Garner, S. Ghosh, A. Mallick, D. Basak, M.F.A.M. Van Hest, High-performance flexible perovskite solar cells on ultrathin glass: implications of the TCO, J. Phys. Chem. Lett. 8 (2017) 4960–4966.

[16] S. Survase, H. Narayan, I. Sulania, M. Thakurdesai, Swift heavy ion irradiation induced nanograin formation in CdTe thin films, Nucl. Instruments Methods Phys. Res. B 387 (2016) 1–9.

[17] A. Morel, Y. Borjon-Piron, R.L. Porto, T. Brousse, D. Bélanger, Suitable conditions for the use of vanadium nitride as an electrode for electrochemical capacitor, J. Electrochem. Soc. 163 (2016) 1077–1082.

[18] N.L. Do, E. Garcia-Caurel, N. Bérerd, N. Moncoffre, D. Gorse - Pomonti, Determination of thicknesses of oxide films grown on titanium under argon irradiation by spectroscopic ellipsometry, J. Nucl. Mater. 447 (2014) 197–207.

[19] M.C. Biesinger, L.W.M. Lau, A.R. Gerson, R.S.C. Smart, Resolving surface chemical states in XPS analysis of first row transition metals, oxides and hydroxides: *sc*, Ti, V, Cu and Zn, Appl. Surf. Sci. 257 (2010) 887–898.

[20] R. Tian, S.H. Park, P.J. King, G. Cunningham, J. Coelho, V. Nicolosi, J.N. Coleman, Quantifying the factors limiting rate performance in battery electrodes, Nat. Commun. 10 (2019).

[21] E. Le Calvez, D. Yarekha, L. Fugère, K. Robert, M. Huvé, M. Marinova, O. Crosnier, C. Lethien, T. Brousse, Influence of ion implantation on the charge storage mechanism of vanadium nitride pseudocapacitive thin films, Electrochem. Commun. 125 (2021) 0–4.